6DOF motion and Cavity Dynamics of a Ventilated Super-cavitating Vehicle with Control Fins

[1]Sungtaek Park; [1]Jeonghwa Seo; [1]Shin Hyung Rhee*; [2]Sangdon Lee;

[1]Seoul National University, Seoul, Korea; [2]NEXTfoam Co., Ltd., Seoul, Korea

Abstract

Flow fields around a super-cavitating vehicle with control fins in ventilated cavity and its six-degrees-of-freedom (6DOF) motion were investigated by computational fluid dynamics (CFD) analysis. SNUFOAM, a CFD program based on an open-source CFD toolkit and specialized for naval hydrodynamics, was used in this study. A mixture fluid-based cavitation model and k - ω SST model were employed for the analysis of turbulent multiphase flow with liquid water, vapor, and non-condensable gas. Convection and diffusion terms were discretized by the second order upwind and central differencing scheme, respectively. The geometry of interest was a super-cavitating vehicle consisted of a cone-shaped nose, cylindrical main body, and four control fins near the tail. A cavitator and ventilation holes for injecting non-condensable gas were located at the nose of the vehicle. To accommodate the motion of deploying fins, a layering mesh technique was employed, while a mesh morphing technique was used for the motion of the vehicle body. Two different control fin operations, which are deploying and deflecting fins, were applied and the effects of injecting non-condensable gas were also examined.

Keywords: Super-cavitation; 6DOF motion; CFD; Ventilated cavitation

Introduction

Super-cavitating underwater vehicles can significantly reduce frictional drag, unlike conventional ones, by generating cavity around the body and achieve high speed. Control fins of a super-cavitating vehicle are partially immersed in the cavity, thus interaction of cavity dynamics and force on the fins should be considered to analyze the maneuverability of the super-cavitating vehicle [1, 2].

For initiating and maintain super-cavitation, cavitation number should be kept sufficiently low. It is tough to achieve and maintain the status by natural cavitation only, and therefore ventilated cavitation by injection of non-condensable gas has been also studied [3]. In those studies, due to extreme difficulty in model testing, CFD analysis is the most feasible method to analyze the cavity dynamics and maneuverability of the ventilated super-cavitation vehicle. The present study aims to introduce CFD methods for a ventilated super-cavitation vehicle and analyze 6DOF motion of the vehicle with fin operation.

Problem Description

The test model was an axisymmetric super-cavitating vehicle. Figure 1 shows the model geometry with a cavitator and six injector holes. Four control fins were attached near the tail. The length (L) and diameter (D) of the model were 2.1 m and 0.145 m, respectively. The span of control fins was 0.128 m and the chord at the fin root was 0.0196 m.
Two conditions of control fin operation, i.e., deploying fins after launching and deflecting fins for maneuvering, were tested. The vehicle advance speed when deploying control fins was 20 m/s. Fins were initially lain in slits on the body and deployed within 0.5 sec after the cavitation surrounding the vehicle was fully developed. The case of deflecting fins assumes that the cavity is fully developed at the design speed 50 m/s. The deflection angle was 1.5°. For both cases, the injection volume of non-condensable gas from ventilation holes was 0.069 m^3/s. No-injection condition was also tested in the fin deflection case.

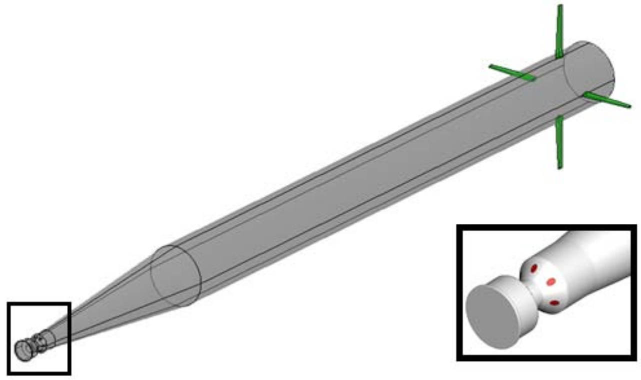

Figure 1 Design of the super-cavitating vehicle

Governing Equations and Numerical Methods

The governing equations of the numerical simulation were the continuity equation and unsteady Reynolds-averaged Navier-Stokes equation. The presence of three phases (water liquid, vapor, and non-condensable gas) was represented by volume fraction.

Computations were carried out using SNUFOAM, which was developed based on an open-source CFD toolkit, OpenFOAM [4]. SNUFOAM employed a cell-centered finite-volume method based on a multi-dimensional linear reconstruction scheme that permitted the use of computational elements (cells) with arbitrary polyhedral cell topology. The solution gradients at cell centers were obtained by applying Green-Gauss theorem based on a node-based quadrature. For discretization of convection terms and diffusion terms in filtered momentum equations, we adopted a quadratic upwind differencing (QUICK) scheme and the second order central-differencing scheme, respectively. The system of discretized governing equations was solved using point-implicit Gauss-Seidel relaxation along with algebraic multi-grid method to accelerate solution convergence. For turbulence closure, the k-ω SST model [5] was used.

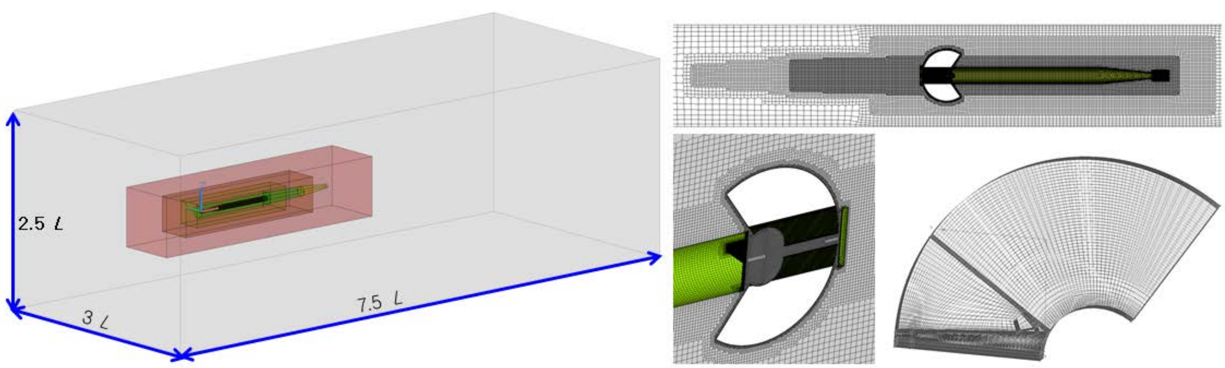

Figure 2 Computational domain and mesh around the vehicle and control fins

Figure 2 shows the computational domain and grids. The upstream inlet and downstream exit boundary was located at 1.5 L forward and 5 L aft from the model, respectively. The width of the computational domain was 3 L and height was 2.5 L. To enable deploying motion of control fins, the layering mesh method was applied. The layering mesh method is effective to analyze a motion of large displacement along a trajectory. Morphing mesh technique was used to analyze 6DOF motion of the vehicle body with small displacement and arbitrary direction. The dynamic mesh zone that morphing was allowed was within 0.75 L from the vehicle body.

Results and Discussion

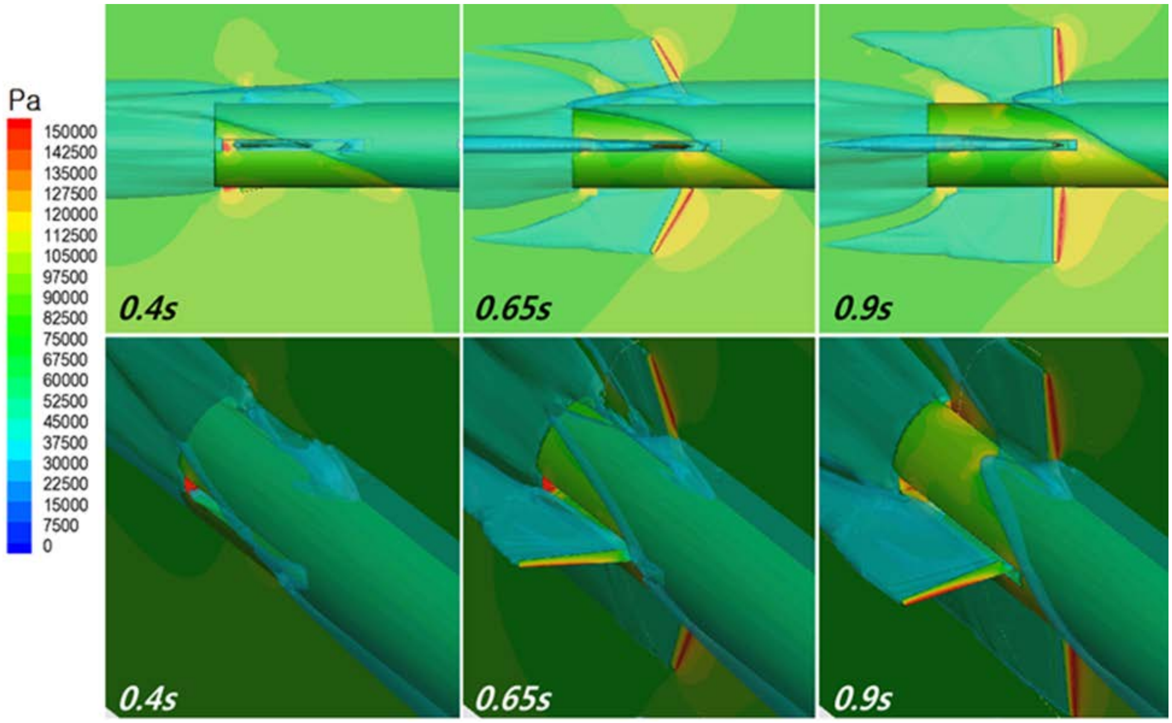

Figure 3 Pressure contours and the boundary of the cavity at deploying control fins in fully developed super-cavitation

Figure 3 shows pressure distribution and cavity shape around the vehicle and control fins during the deploying phase. The cavity was generated from the nose with small local cavities were observed behind the fins and body. Owing to the buoyancy of the non-condensable gas, the cavity on the upper side was larger than that on the lower side. At 0.3 s, the super-cavitation was fully developed and the control fins began to deploy. Drag force on control fins increased as they were unfolded. At 0.8 s, the control fins were completely deployed and the drag force was converged (see Figure 4). The asymmetry of the cavity resulted in imbalance of drag force on the control fins. Drag force on the top fin was smaller than that on the bottom fin, but showed fluctuation after 0.8 s, due to tail slap on the cavity boundary.

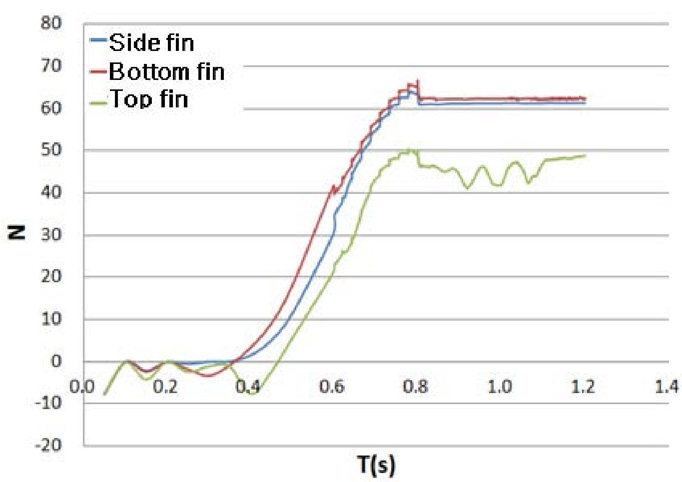

Figure 4 Drag on the control fins at deployment

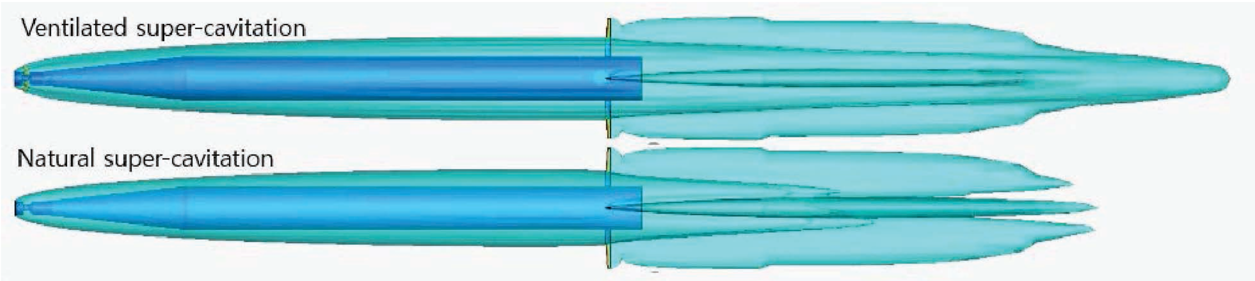

Figure 5 Cavity around the super-cavitation vehicle

Figure 5 shows fully developed cavity around the test model before fin deflection at advance speed of 50 m/s. With the ventilated super-cavitation case, the cavity was thicker than that with the natural case, resulting in different immersed depth of the fins. In both of cases, the gravity caused a bias of cavity toward the upward direction, but the ventilation case with non-condensable gas injection showed more severe bias, and the resultant pitching moment on control fins was generated.
For maneuvering of the super-cavitating vehicle, top and bottom fins were deflected by 1.5° to cause yaw motion. Figure 6 shows time history of roll and yaw motion of the vehicle. Deflection of control fins began at 0 s. At 0.1 s, yaw motion fluctuated as the tail slapped the cavity boundary, but increased gradually from 0.2 s.
Roll motion of the vehicle was also observed, because of different immersed depth of the top and bottom fins. Lift on the bottom fin was larger than that on the top fin, and the imbalance of lift resulted in roll moment on the vehicle body caused roll motion. The ventilated cavitation case, where the imbalance was larger, showed greater change of roll motion.

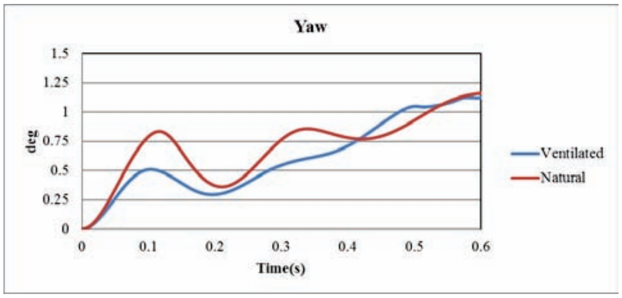

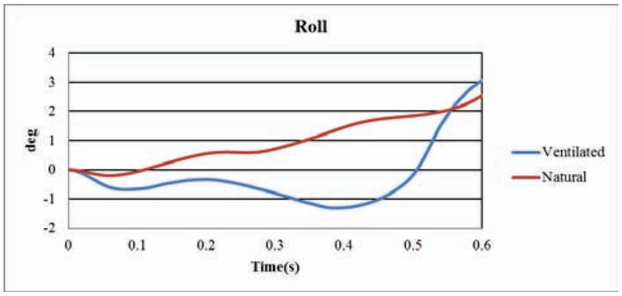

Figure 6 Time history of the motion of the super-cavitating vehicle

Conclusion

Mesh morphing technique in a multi-phase flow CFD solver was applied to analyze flow fields around a super-cavitating vehicle with control fins deployment and deflection. The ventilated cavitation was asymmetric and skewed upward. Tail slap and fluctuation of drag on the top fin were observed. For fin deflection, effects of non-condensable gas injection were examined. Ventilated super-cavitation case showed less fluctuation in yaw motion, but greater change in roll motion than natural super-cavitation.

References

[1] Lin, G., Balachandran, B., Abed, E. H. (2007). *Nonlinear dynamics and bifurcations of a supercavitating vehicle.* IEEE Journal of Oceanic Engineering. 32(4).
[2] Lin, G., Balachandran, B., Abed, E. H. (2008). *Dynamics and control of supercavitating vehicles.* Journal of Dynamic Systems, Measurement, and Control. 130(2).
[3] Lindau, J. W., Kunz, R. F., Boger, D. A., Stinebring, D. R., Gibeling, H. J. (2002). *High Reynolds number, unsteady, multiphase CFD modeling of cavitating flows.* Journal of Fluids Engineering. 124(3).
[4] Jasak, H. (2009). *OpenFOAM: Open source CFD in research and industry*. International Journal of Naval Architecture and Ocean Engineering. 1(2).
[5] Menter, F. R. (1994). Two-equation eddy-viscosity turbulence models for engineering applications. AIAA Journal. 32(8).